Water Science & Technology

IWA PUBLISHING

Water Science & Technology Vol 87 No 4, 823 doi: 10.2166/wst.2023.033

Implementation of an anaerobic selector step for the densification of activated sludge treating high-salinity petrochemical wastewater

Sven Poelmans, Lennert Dockx, Karina Seguel Suazo, Dorothee Goettert and Jan Dries *

Faculty of Applied Engineering, Research Group Biochemical Wastewater Valorization and Engineering (BioWAVE), University of Antwerp, Groenenborgerlaan 171, Antwerp 2020, Belgium
*Corresponding author. E-mail: jan.dries2@uantwerpen.be

SP, 0000-0002-0236-0400; LD, 0000-0003-2698-7985; DG, 0000-0003-4941-4901; JD, 0000-0002-0204-5697

ABSTRACT

Sludge bulking is a common challenge in industrial biological wastewater treatment. Leading to difficulties such as bad sludge settling and washout, which is a problem also encountered in the petrochemical industry. Anaerobic feeding strategies can be used to induce the growth of storage-capable organisms, such as glycogen-accumulating organisms (GAO), leading to denser sludge flocs and better settling. In this study, the implementation of an anaerobic feeding strategy was investigated for high-salinity petrochemical wastewater ($\pm$35 g salts·L^{-1}), using a sequencing batch reactor. Influent, effluent and sludge characteristics were analyzed throughout the operational period, which can be divided into three stages: I (normal operation), II (increased influent volume) and III (longer anaerobic mixing). Good effluent quality was observed during all stages with effluent chemical oxygen demand (COD) < 100 mgO_2·L^{-1} and removal efficiencies of 95%. After 140 days, the sludge volume index decreased below 100 mL·g^{-1} reaching the threshold of good settling sludge. Sludge morphology clearly improved, with dense sludge flocs and less filaments being present. A maximum anaerobic dissolved oxygen carbon (DOC) uptake was achieved on day 80 with 74% during stage III. 16S rRNA amplicon sequencing showed the presence of GAOs, with increasing relative read abundance over time from 1 to 3.5%.

Key words: anaerobic selector, glycogen-accumulating organisms, high salinity, petrochemical wastewater, sludge bulking, sludge densification

HIGHLIGHTS

- Dense and compact sludge flocs were achieved under high-saline conditions
- Filamentous organisms were suppressed in the system, favoring the growth of glycogen-accumulating organisms
- Settling characteristics of the sludge were improved to the point of the sludge being characterized as well-settling

GRAPHICAL ABSTRACT

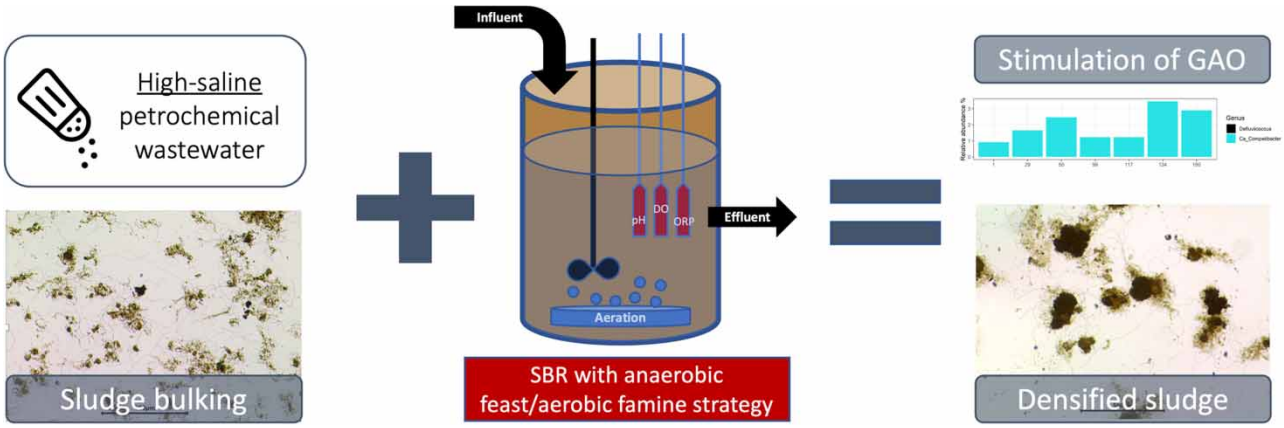

1. INTRODUCTION

A primary and long-standing problem in industrial biological wastewater treatment is bulking sludge. This phenomenon commonly leads to bad sludge settling characteristics, sludge washout and effluent discharge problems. The extensive growth of filamentous organisms is seen as one of the main causes of bulking sludge, leading to the specific terminology of filamentous bulking sludge. As described by Jenkins *et al.* (2003) and Martins *et al.* (2004), different aspects such as low nutrient, substrate or oxygen concentrations, can provoke the extensive growth of filaments, with the organisms forming a net-like structure hindering the settling of sludge. Bulking sludge is a problem that widely occurs in many industries, as a study by Cornelissen *et al.* (2018), conducted in Flanders (Belgium), showed. In this study, 36% of the treatment plants investigated experienced bulking sludge, including plants in the (petro)chemical industry.

Many strategies have been applied to overcome this problem, one being the anaerobic feast/aerobic famine feeding strategy, thus implementing an anaerobic selector. This strategy relies on the selection of slow-growing organisms such as polyphosphate accumulating organisms (PAOs) and glycogen-accumulating organisms (GAOs), another key for the successful formation of aerobic granular sludge (AGS) (de Kreuk & van Loosdrecht 2004; Caluwé *et al.* 2022). These storage organisms are able to store carbon (e.g. volatile fatty acids (VFA)) as storage polymers under anaerobic/anoxic conditions, giving them a clear advantage over filamentous organisms. Ultimately, filaments will be out selected, giving way to the formation of more dense and settleable sludge flocs (and even granules), and hereby improving sludge settling and effluent discharge. The feast/famine strategy has been applied successfully before with various industrial wastewaters. Caluwé *et al.* (2017) were able to improve the sludge characteristics of sludge originating from a petrochemical company. Through the implementation of an anaerobic feast/famine regime for the treatment of petrochemical wastewater, the sludge volume index (SVI) was decreased from 285 to 56 $mL \cdot g^{-1}$ after 30 days. Other industries where the same strategy has been successfully implemented include the tank truck cleaning industry (Caluwé *et al.* 2018, 2022), the potato processing industry (Dobbeleers *et al.* 2017) and breweries (Corsino *et al.* 2017).

Salinity effects on the formation and stability of AGS or dense sludge flocs in general have been widely described, including the effects on the metabolism of PAOs and GAOs, mostly on the basis of NaCl salinity. Pronk *et al.* (2014) investigated the influence of increasing salinity on AGS in a sequencing batch reactor (SBR), where starting at concentrations of 20 g $Cl^{-} \cdot L^{-1}$, the granule size decreased and inhibition of nitrite oxidation occurred which ultimately led to the inhibition of phosphate removal by PAOs. Welles *et al.* (2014) described the short-term influence of Cl^{-} salinity on the anaerobic metabolism of PAOs and GAOs, showing a 71 and 41% decrease, respectively, in the acetate uptake rate when increasing from 0 to 10 g $Cl^{-} \cdot L^{-1}$. While the anaerobic energy requirements increased by 4%, the GAOs seemed to be less influenced by higher NaCl salinity.

The impact of salinity as NaCl has been investigated in great detail, but only a little research is available on the effect of a real salt matrix (e.g. seawater) on PAOs, GAOs and in general the AGS formation processes. In comparison to Pronk *et al.* (2014), de Graaff *et al.* (2020a) showed stable PAO activity when cultivating AGS using artificial seawater (salinity of 35 $g \cdot L^{-1}$), a high enrichment of the PAO '*Ca.* Accumulibacter' and a complete absence of GAOs. In the research of Ramos *et al.* (2015) on the other hand, where saline industrial wastewater was mimicked through the addition of a salt mixture, increasing salt concentrations up to 29 $g \cdot L^{-1}$ were applied to treat aromatics-based wastewater with AGS. An initial acclimation to the salinity and complete biodegradation was observed, but at the highest salt concentrations, a complete deterioration of granules was observed.

While there are a few studies where artificial seawater was used, only a minor amount of research is available on the treatment of real industrial saline wastewaters with AGS, and operated using a feast/famine regime. Carrera *et al.* (2019) investigated the SBR treatment of fish-canning wastewater (salinity up to 13.45 g $NaCl \cdot L^{-1}$), where fast and relatively stable granulation was achieved, with GAOs being dominant in the granules. Pilot-scale experiments with saline (up to 14.35 g $NaCl \cdot L^{-1}$) fish-canning wastewater were examined in follow-up research (Carrera *et al.* 2021), where granulation and good settleability were achieved after 30 days using an anaerobic feast/aerobic famine strategy.

Although knowledge is available on using feast/famine strategies to treat certain high-salinity complex wastewaters, it is still missing on the use of this strategy for high-saline petrochemical wastewater. Therefore, the present research is aimed at the treatment of high-salinity petrochemical wastewater (average salinity of 35 g $salts \cdot L^{-1}$) with an anaerobic feast/aerobic famine process in order to promote sludge densification combined with high removal rates of chemical oxygen demand (COD) and nutrients. Laboratory-scale SBR experiments were conducted with analysis of the activated sludge (settling,

morphology, biomass) and a subsequent determination of the microbial community through 16S rRNA amplicon sequencing to address the influence of salinity on the growth of storage-capable organisms.

2. MATERIALS AND METHODS

2.1. Reactor set-up

A laboratory-scale SBR with a working volume (before feeding) of 11 L was used in this study. The SBR was equipped with a mixer (Heidolph, Germany) to keep the sludge in suspension, an influent feeding pump (Iwaki, Germany) and a discharge valve. Oxygen was supplied to the mixed liquor by an AquaForte aeration pump, connected to a ceramic disk diffuser. The aeration was done between two setpoints, with a subsequent calculation of the oxygen uptake rates (OUR) within each decrease in oxygen concentration. The oxygen, pH and redox potential (ORP) were constantly monitored through an optical dissolved oxygen sensor (Jumo ecoLine O-DO B202613, Jumo, Germany), pH sensor (Jumo tecLine 201021, Jumo, Germany) and ORP sensor (Jumo tecLine 201026, Jumo, Germany), respectively. Data logging of the sensors was done using an Aquis Touch S system (Jumo, Germany). General communication and operation with/of the reactor system was done using LabView™-software (National Instruments, USA) through a data acquisition card (National Instruments, USA).

2.2. Reactor operation

The SBR was inoculated with seed sludge originating from a petrochemical company and subsequently fed with the wastewater from the same company. The reactor was operated for 150 days with an SBR cycle of 12 h. A standard cycle consisted of several steps, including an anaerobic feeding step, applying the anaerobic feast/aerobic famine method to induce the growth of slow-growing organisms such as GAO. The anaerobic feeding step was split into a non-mixed and mixed phase, then followed by an extended anaerobic mixing step, an aerobic period with aeration between 1 and 3 mg $O_2 \cdot L^{-1}$, and ultimately settling and effluent discharge steps. Throughout the operational period of the SBR, three periods or stages can be distinguished where changes to the cycle were made. During stage I (days 1–21), 1 L of influent was fed per cycle; during stage II (days 21–73), the influent volume was increased to 1.5 L per cycle; and during stage III (days 73–150) the length of the anaerobic mixing period, which follows the feeding step (1.5 L influent/cycle), was increased by 30 min to promote substrate uptake. The different times of each cycle step can be found in Table 1 for all three stages.

A constant temperature of 25 °C was used throughout the reactor operations. Additionally, during stage III, excess sludge was periodically withdrawn to maintain a constant sludge retention time (SRT) of 50 days. A schematic overview of the SBR cycle and set-up can be found in the Supplementary Information S1.

2.3. Industrial wastewater

Nutrient-limited wastewater (COD:N:P = 100:2.35:0.01) from a petrochemical company was used, with different batches (collected at the company at different timepoints) being fed to the reactor during the operational period of 150 days. The average concentration of the wastewater is shown in Table 2, showing the variation of the influent. Concentrations of Cl^-, SO_4^{2-} and Na^+ were also determined, being 18, 5 and 10 $g \cdot L^{-1}$, respectively. Combined with high electrical conductivity (EC) values, the wastewater can therefore be classified in the category of seawater (30–35 g salts$\cdot L^{-1}$). Nutrients were dosed (as NH_4Cl and K_2HPO_4 solutions) in the wastewater when nutrient requirements for optimal growth were not met (to a COD:N:P ratio of 100:3.5:0.4) based on Hamza *et al.* (2019) and preliminary research.

Table 1 | Overview of SBR cycle times during different stages of operational period

	Stage I (day 1–21)	Stage II (day 21–73)	Stage III (day 73–150)
Feeding (not mixed)	30 min	45 min	45 min
Feeding (mixed)	30 min	45 min	45 min
Anaerobic mixing	210 min	180 min	210 min
Aerobic step	320 min	320 min	290 min
Settling	120 min	120 min	120 min
Discharge	5 min	5 min	5 min
Total cycle time	**12 h**	**12 h**	**12 h**

Table 2 | Average influent wastewater characteristics

Parameter	Value (±standard deviation)
COD (mg COD L^{-1})	2,010 (± 426)
sCOD (mg sCOD L^{-1})	1,800 (± 535)
DOC (mg C L^{-1})	547.9 (± 72.6)
NH_4-N (mg NH_4-N L^{-1})	15.38 (± 8.12)
Total N (mg total N L^{-1})	48 (± 21)
PO_4-P (mg PO_4-P L^{-1})	0.28 (± 0.25)
Volatile fatty acids (mg VFA L^{-1})	609 (± 127)
pH (–)	8.00 (± 0.39)
Electrical conductivity (EC, mS cm^{-1})	53.13 (± 3.91)

2.4. Analysis of the influent, effluent and activated sludge

The influent and effluent waters were characterized using the following parameters: total COD, soluble COD (sCOD), DOC, NH_4^+-N, NO_2^--N, NO_3^--N, total N, PO_4^{3-}-P, pH and electrical conductivity (EC). VFA, chloride (Cl^-), sulfate (SO_4^{2-}) and sodium (Na^+) concentrations were only determined for influent. COD and sCOD measurements of influent samples were conducted with a Hanna Instruments (Temse, Belgium) COD Medium Range test kit (HI93754B, accuracy of ± 15 mg $O_2 \cdot L^{-1}$) with sufficient dilution to avoid chloride interference. The COD and sCOD of the effluent samples were measured with a Nanocolor COD 60 (Machery-Nagel, accuracy of ± 3.87 mg $O_2 \cdot L^{-1}$) test kit using a Nanocolor chloride complexing agent (Machery-Nagel) to increase the chloride interference range and to minimize the dilution for lower COD-values. NH_4^+-N, NO_2^--N, NO_3^--N and PO_4^{3-}-P were analyzed using Hanna Instruments test kits HI93715, HI93707, HI93766 and HI93717, respectively. Accuracies for the used test kits were ± 0.05 mg $N \cdot L^{-1}$ for NH_4^+-N, ± 20 µg $N \cdot L^{-1}$ for NO_2^--N, ± 1,0 mg $N \cdot L^{-1}$ for NO_3^--N, ± 1.0 mg $P \cdot L^{-1}$ for PO_4^{3-}-P. The DOC was measured with a Sievers InnoVox Laboratory Total Organic Carbon Analyser. The pH and conductivity were measured using a HI99141 portable meter and a HI99301 N portable meter (Hanna Instruments), respectively. VFA, Cl^- and SO_4^{2-} were measured with the following test kits; LCK-365 (Hach), HI3815 (Hanna Instruments) and SulfaVer 4 powder pillows (Hach), respectively. Na^+ concentrations were provided by the petrochemical company. For all the above-mentioned tests, except for the total COD, filtered samples (through 1.2 µm glass microfiber filters) were used.

Activated sludge was characterized through biomass measurements as mixed liquor suspended solids (MLSS) and mixed liquor volatile suspended solids (MLVSS), and sludge settling using the SVI, including a diluted (4×) SVI, shown as dSVI. The sludge morphology was followed through brightfield microscopy using an Olympus CX43 Biological Microscope (Olympus, Japan). (d)SVI, MLSS and MLVSS were measured according to the APHA Standard Methods for Examination of Water and Wastewater (APHA 2017).

2.5. *In situ* cycle measurements

In situ cycle measurements were conducted to provide insight into the anaerobic carbon uptake in the SBR system. Samples were taken for DOC analysis during one cycle of the reactor, more specifically during the anaerobic feeding step and the anaerobic mixing step. The uptake of DOC was calculated using the following equation:

$$\%\ \text{DOC uptake (anaerobic)} = \frac{(V_{inf} * C_{inf}) - (V_{SBR,An} * C_{SBR,An}) - (V_{SBR,end} * C_{SBR,end}) - DOC_{NOx}}{(V_{inf} * C_{inf})} \quad (1)$$

with V_{inf}, $V_{SBR,An}$ and $V_{SBR,end}$ being the volumes (in L) of the influent fed to the reactor, in the SBR at the end of the anaerobic mixing step and in the SBR at the end of the previous cycle, respectively. C_{inf}, $C_{SBR,An}$ and $C_{SBR,end}$ are the DOC concentrations (in mg $C \cdot L^{-1}$) of the influent feed, in the SBR at the end of the anaerobic mixing step and in the SBR at the end of the previous cycle, respectively. Within the calculation, any DOC usage due to denitrification is subtracted

from the total DOC uptake. The denitrification usage of DOC (DOC_{NOx} in mg C) was calculated using the following equation:

$$DOC_{NOx} = ((V_{inf} * C_{NOx,inf}) + (V_{SBR,end} * C_{NOx,SBR,end})) * \left(\frac{COD}{NO_x - N}\right) * \left(\frac{DOC}{COD}\right) \quad (2)$$

with $C_{NOx,inf}$ and $C_{NOx,SBR,end}$ being the concentration of nitrate/nitrite in the influent and in the SBR at the end of the previous cycle, respectively (in mg NO_3-N·L^{-1} or mg NO_2-N·L^{-1}). For NO_3-N, a COD/NO_x-N ratio of 4 was used, while for NO_2-N, a COD/NO_x-N ratio of 2.4 was used, based on Chung & Bae (2002) and Chiu & Chung (2003). A DOC/COD conversion factor was used to convert COD to DOC based on the DOC/COD ratio of the used influent.

2.6. 16S rRNA gene amplicon sequencing

Biomass samples were collected weekly, typically at the end of each cycle, then centrifuged with the resulting pellet being stored at −20 °C prior to DNA extraction. DNA was isolated using the FastDNA® SPIN kit following the van Loosdrecht *et al.* (2016) protocol. The DNA concentration was then measured using the Qubit dsDNA Assay kit (Invitrogen, USA), following the manufacturer's protocol.

The bacterial 16S rRNA gene hypervariable region, targeting V1–3, was amplified through a polymerase chain reaction (PCR). Barcoded primers were used 27F (5′-AGAGTTTGATCCTGGCTCAG-3′), 534R (5′-ATTACCGCGGCTGCTGG-3′), and KAPA HiFi HotStart PCR kit (Boston, USA). PCR products were purified using the Agent AMPure XP Beads kit, following the manufacturer's protocol, and then pooled into one library. The resulting library had a final equimolar concentration of 4 nM. The sequencing of the amplified libraries was carried out on an Illumina MiSeq platform at the Center for Medical Genetics (Edegem, Belgium), using a MiSeq Reagent kit v (Illumina), following standard guidelines. The reads were clustered using the USEARCH v.11.0.667 (Edgar 2013) toolbox and taxonomically classified with the MiDAS 4 database (Dueholm *et al.* 2022). Amplicon sequencing data analysis was performed using the ampvis2 package v. 1.24.0.

3. RESULTS AND DISCUSSION

3.1. General reactor performance

During stages I and II of the study, a good effluent quality in terms of COD was achieved, with COD and sCOD ending below 150 and 100 mg O_2·L^{-1}, respectively (Figure 1). During stage III, a temporary increase in both sCOD and COD was observed, with a higher influent COD being the most probable cause of increasing the recalcitrant fraction. Overall, an average COD removal efficiency of 95 ± 1% was achieved. During the anaerobic feeding strategy used by Carrera *et al.* (2019) with saline fish-canning wastewater (varying salinity of 4.97–13.45 g NaCl·L^{-1}), COD removal efficiencies around 80% were achieved. In a study by Wang *et al.* (2017a), where the impact of different salinities (NaCl) was tested on AGS stability with synthetic saline wastewater, an increasing *NaCl salinity* from 5 to 15 g L^{-1} significantly decreased the COD removal rates from 92.38 to 55.92%, respectively. This is in contrast with the present study, where the system, already acclimated to high salt concentrations of >15 g L^{-1}, showed high removal rates in all stages.

Figure 1 also shows the food to microorganisms ratio (F/M ratio) over time for the working period of the reactor. The F/M ratio shows the amount of food available (as COD) for the amount of microorganisms (as MLVSS) present, giving a glance at COD loading of the activated sludge. During stage I, an average F/M of 0.18 ± 0.02 gCOD·$gVSS^{-1}$·d^{-1} was achieved, with a corresponding organic loading rate (OLR) of 0.41 ± 0.01 kgCOD·m^{-3}·d^{-1}. The stable OLR was achieved due to the same influent being used during the first 20 days of operation. With higher influent variability and an increased feeding volume during stage II, the average F/M increased to 0.20 ± 0.03 gCOD·$gVSS^{-1}$·d^{-1}, with a respective average OLR of 0.50 ± 0.06 kgCOD·m^{-3}·d^{-1}. During stage III, with an increase in the length of the anaerobic mixing phase, a much lower average F/M of 0.15 ± 0.02 gCOD·$gVSS^{-1}$·d^{-1} was observed with a clear decrease during the period overall (Figure 1). The respective OLR was higher compared to stages I and II, at 0.57 ± 0.08 kgCOD·m^{-3}·d^{-1}, with a higher biomass concentration (section 3.2) causing the lower F/M ratio. Overall, the OLR in this study was lower than that used by Carrera *et al.* (2019) who used saline fish-canning wastewater, with the lowest used OLR at 1.8 kgCOD·m^{-3}·d^{-1}. van den Akker *et al.* (2015) on the other hand, used a more comparable OLR between 0.98 and 1.55 kgCOD·m^{-3}·d^{-1}, achieving 98% BOD_5 removal treating saline municipal sewage (5.3–6.1 g NaCl·L^{-1}) with AGS.

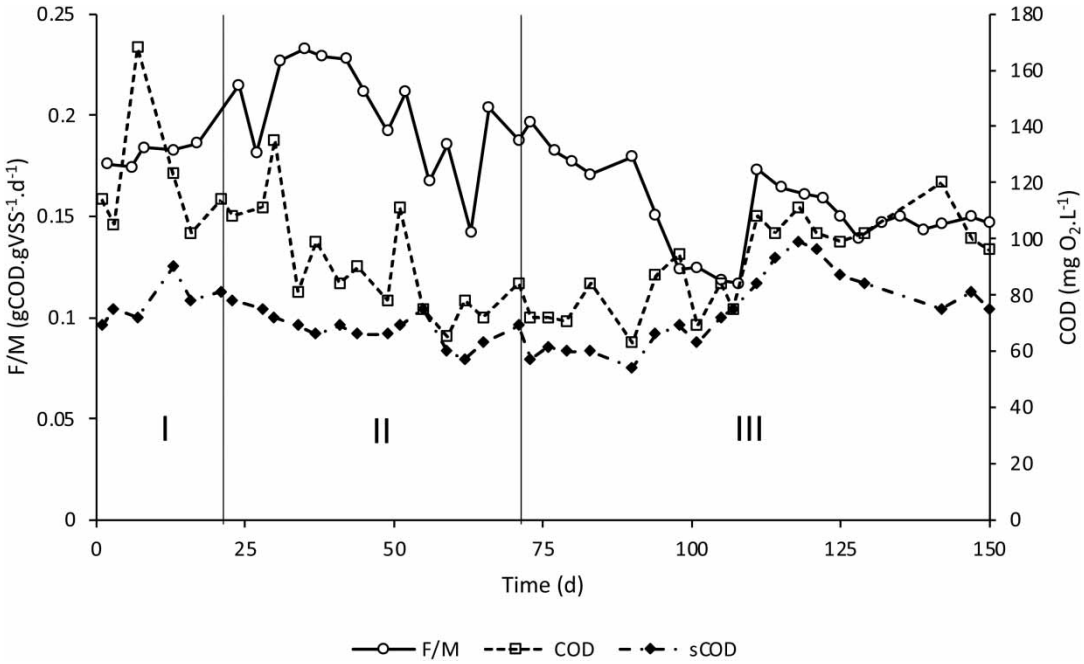

Figure 1 | Overall reactor performance with evolution of effluent COD, effluent sCOD and F/M over time, shown at stages I, II and III.

3.2. Sludge characteristics

The main aim of the present study was to achieve well-settling sludge and to induce the growth of GAOs to significantly change the sludge morphology. The settling time was kept at 2 h, due to the initial poor settling of the sludge, and to achieve sludge densification purely with microbial selection (feast/famine). High salinity was treated as the challenging factor in achieving better sludge characteristics. The evolution of the MLSS in the reactor and the sludge settling characteristics as diluted SVI_{30} ($dSVI_{30,}$ the dSVI after 30 min) are shown in Figure 2. The MLSS showed a stable evolution during stages I and II, giving an average of 3 $g{\cdot}L^{-1}$ (Figure 2). Near the end of stage II, around day 50, the MLSS started to increase to

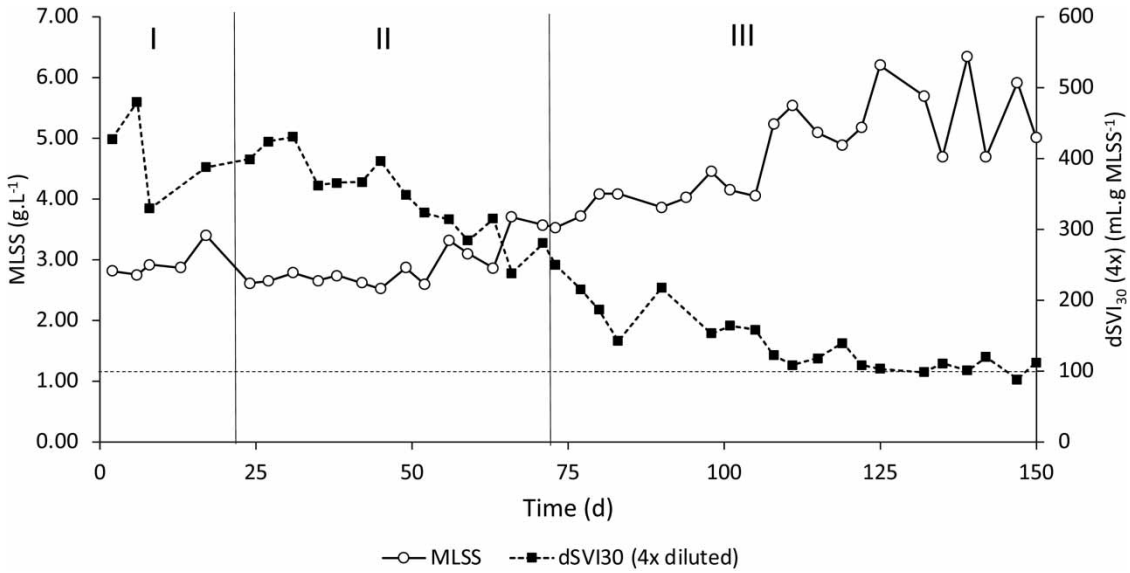

Figure 2 | Evolution of mixed liquor suspended solids (MLSS) and diluted sludge volume index (dSVI) during the working period of the reactor; dashed horizontal line shows the threshold of $dSVI_{30}$ at 100 $mL{\cdot}gMLSS^{-1}$.

3.5 g·L^{-1}. The higher feeding volume of 1.5 L could have led to an increase in biomass growth. This increase continued into stage III, where the anaerobic mixing time after feeding was increased by 30 min. This may have given the sludge an adaptation period for the complex petrochemical matrix. The prolongation gives extra time for complex substrates to be hydrolyzed during the anaerobic phase before being taken up anaerobically, mostly as VFAs, which are taken up by the GAOs. The hydrolysis of more complex and polymeric substrates has been described by Toja Ortega *et al.* (2021) and de Kreuk *et al.* (2010) for AGS. During stage III, sludge was discharged to achieve an SRT of 50 days, with the MLSS finally stabilizing around day 125 at 5 g·L^{-1}, small fluctuations were observed; however, this was due to the inorganic salt fraction present in the mixed liquor. Biomass concentrations (as MLVSS) reached a stable value in stage III around 4 g·L^{-1} by day 120.

Sludge settling (as $dSVI_{30}$ in Figure 2) started on the higher end, with $dSVI_{30}$ between 400 and 500 mL·gMLSS^{-1}, being categorized as poorly settling sludge. During stage II, a small increase in the $dSVI_{30}$ was observed, shifting to a steady decrease starting around day 30, and ultimately reaching 280 mL·g^{-1} after 70 days of operation. This suggests that the higher feeding volume had an influence on sludge densification. The decreasing SVI trend continued in stage III, where the prolonged anaerobic mixing period further induced the formation of dense sludge flocs with $dSVI_{30}$ reaching its lowest value of 88 mL·g^{-1} at day 147. By reaching the threshold of 100 mL·g^{-1} towards the end of the experiment, the sludge could be classified as well-settling, showing the feasibility of sludge densification by using anaerobic feast/aerobic famine in the presence of high salinity. Looking at the fish-canning industry, Carrera *et al.* (2019) with a starting SVI_{30} of 300 mL·g^{-1}, were able to achieve a decrease in SVI_{30} ending up below 50 mL·g^{-1} and below 100 mL·g^{-1} after 150 days using a short anaerobic feeding with aerobic reaction and plug-flow anaerobic feeding, respectively. This is comparable to the settling properties achieved in the present study. Similar results were achieved by Carrera *et al.* (2021) at a pilot-scale. This clearly indicates that problems caused by salinity can be overcome to achieve good sludge settling, as similar results were also achieved in different studies (Ramos *et al.* 2015; van den Akker *et al.* 2015; Ou *et al.* 2018).

When investigating the sludge morphology (Figure 3), the following pattern could be observed. In the seeding sludge, small and open flocs were observed, with an abundant presence of filamentous organisms. When moving to the end of stage II, a clear densification of sludge flocs could be seen, with filaments still present although at a lower quantity. By day 150, dense and well-defined sludge flocs could be observed despite the presence of filaments, which is in line with the low SVI's, clearly showing the success of the densification strategy with high-salinity petrochemical wastewater. As a comparison, de Graaff *et al.* (2020b) were able to achieve stable granulation, while including the filamentous organism *Thiotrix* using synthetic seawater.

3.3. Anaerobic uptake and GAO population

To assess the evolution of the anaerobic storage capabilities of the activated sludge in the system, *in situ* cycle measurements were conducted to follow DOC uptake during the anaerobic feeding and mixing period. Figure 4(a) shows the anaerobic DOC uptake over time, including the respective VFA percentages of the influent wastewater. During stages I and II, a relatively low average DOC uptake of 23 ± 9% was observed, with DOC consumption through denitrification already accounted for. The lowest uptake at 8% was observed on day 65, when high amounts of nitrite in the influent wastewater (±30 ppm NO_2^--N)

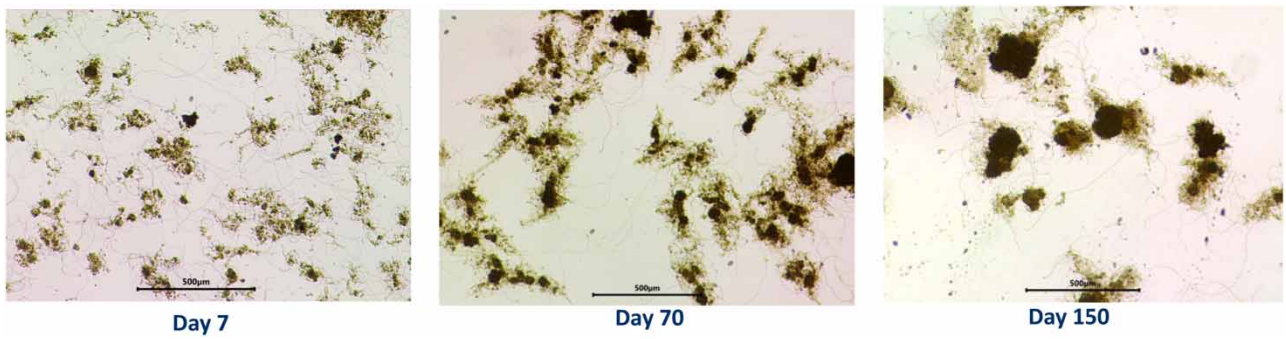

Figure 3 | Evolution of the sludge morphology through brightfield microscopy images for days 7, 70 and 150 at × 2 magnification, scale bars = 500 μm.

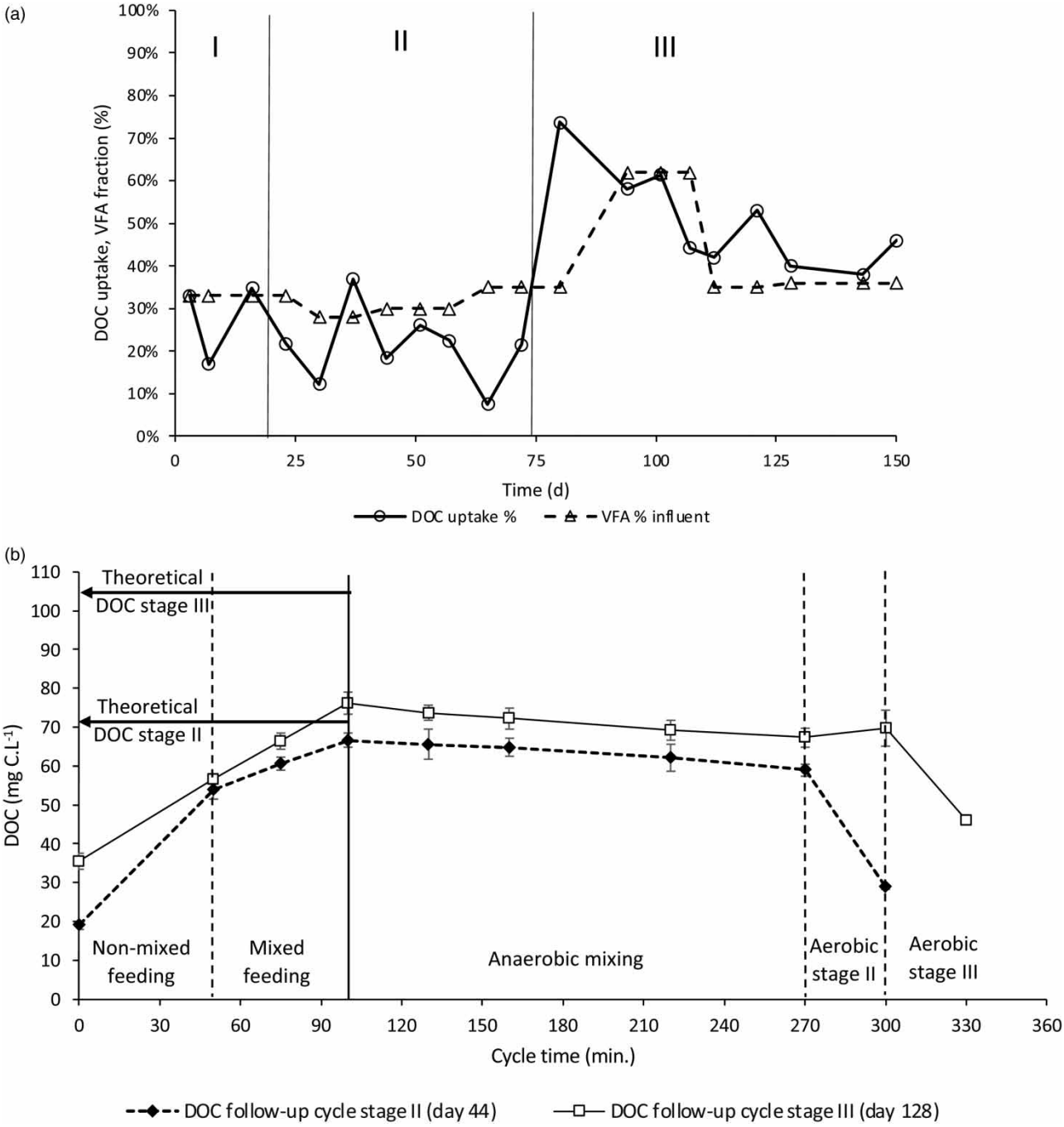

Figure 4 | Evolution of anaerobic DOC uptake (%) during reactor operation, including %VFA in the respective influent wastewater during each specific period (a) and detailed *in situ* cycle measurements showing DOC changes during a cycle in stage II, day 44 and stage III, day 128 with theoretical expected DOC values for each cycle (b).

caused little DOC to be available for uptake by storage organisms (GAOs). During stages I and II, 30% of the influent COD was present as VFAs, which are easily taken up anaerobically. At the beginning of stage III, a sharp increase in DOC uptake was observed, reaching a maximum value of 74%, with VFAs being present at 35% in the influent. This increase coincides with the increased anaerobic mixing time, introduced at day 70. The relatively high uptake percentage suggests that the longer mixing period may contribute to higher COD hydrolysis rates, making more substrate available for storage-capable organisms during the anaerobic phase. The anaerobic uptake decreased after day 80, ultimately leading to a DOC storage

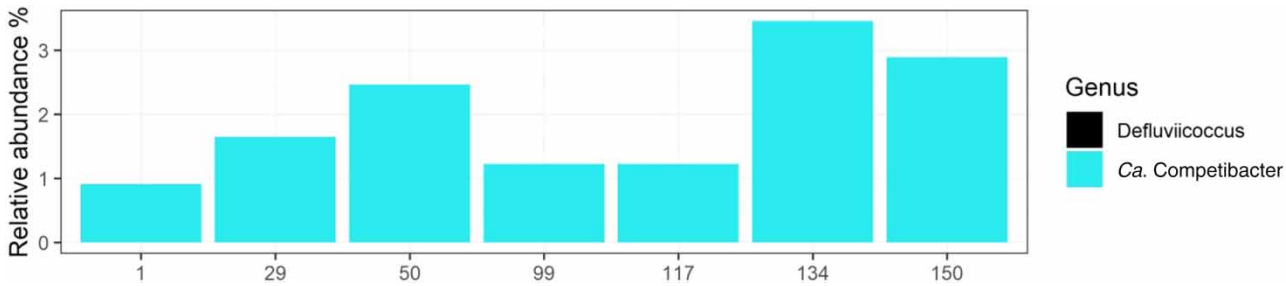

Figure 5 | Evolution of the GAO population (as relative read abundance) for the activated sludge during reactor operation (as days).

of 46% by day 150. This stabilization coincides with both increases (to 60%) and decreases (to 35%) of the VFA content, making it clear that VFAs are not the only driving force, but that the hydrolysis of not-readily storable COD may also play a role.

Figure 4(b) shows an overview of two *in situ* cycle measurements with the changing DOC concentrations for a cycle during stage II and a cycle during stage III (with additional anaerobic mixing time). Anaerobic DOC uptake percentages were 18 (stage II, day 44) and 40 (stage III, day 128) with %VFA being 30 and 36, respectively. Both cycle measurements showed a steady DOC increase during feeding. During the anaerobic mixing periods, both in stage II and stage III, a decrease in DOC was observed, which can mainly be attributed to anaerobic uptake. The additional 30 min mixing time did not show a clear additional decrease in DOC during measurements, although a higher anaerobic uptake was observed. Most of the anaerobic uptake already happened during the (mixed) feeding step. This could be concluded by taking into account the theoretical DOC value that was expected at the end of feeding (Figure 4(b)). As this is mainly through the uptake of VFAs, the DOC decrease during the anaerobic mixing phase was less steep. Since not all DOC was taken up anaerobically, a part of the DOC was still available for filamentous (and other ordinary heterotrophic) organisms to grow during the aerobic phase, probably explaining the presence of filaments even when dense sludge structures were achieved (Figure 3).

During the reactor operation, samples were taken regularly to assess the microbial community through 16S rRNA amplicon sequencing. Due to many unknown genera being present in the sludge matrix because of the specific high-salinity and petrochemical matrix, only the evolution of the GAO population is presented. PAOs are not shown, as relative read abundances $<0.8\%$ were observed throughout the entire period. Although clearly present in microscopy pictures, read abundances for filamentous organisms were observed to be $<1\%$ during the experiment and are also not shown, with possibly the high number of unknown genera ($>50\%$) as a cause of these low percentages. Figure 5 shows the evolution of the GAO '*Ca.* Competibacter' as relative read abundances. A relatively low read abundance of '*Ca.* Competibacter' was observed at reactor startup, accounting for only 1%. Even though relatively low abundances were recorded due to the large unknown microbial matrix, an increase in the relative read abundance to a maximum of 3.5% was observed. Due to the MiDAS 4 database covering taxonomy data from samples taken mainly at wastewater plants with low or medium industrial loads (Dueholm *et al.* 2022), it is possible that other GAO-like organisms were present in the sludge but were not detected through the database. The increase in relative read abundance for '*Ca.* Competibacter' indicates that the enrichment of GAOs happened in the system, even under the high-salinity circumstances, confirming the densification of the sludge and the improvement in settling characteristics seen throughout the operating period of the reactor. The presence of GAOs and PAOs in saline environments was reported in several studies with Carrera *et al.* (2019) showing GAO abundances above 30%, but no presence of PAOs (through FISH analysis) and de Graaff *et al.* (2020b) showing the presence of the PAO '*Ca.* Accumulibacter' around 50% in seawater adapted granules but the absence of any GAOs. Other studies showing the resistance of GAOs to these (high) saline conditions (Welles *et al.* 2014; Wang *et al.* 2017b; He *et al.* 2020) further confirm the results in the present study.

4. CONCLUSIONS

Successful densification of activated sludge treating high-salinity petrochemical wastewater could be achieved in this study. High COD removal rates (95%) were achieved, with effluent discharge limits being met. In terms of settling characteristics, well-settling sludge ($dSVI_{30} < 100\ mL{\cdot}g^{-1}$) was observed at the end of the operational period with clear densification of sludge flocs observed by microscopy analysis. The presence of the GAO '*Ca.* Competibacter' was confirmed through 16S

rRNA amplicon sequencing, showing the resistance of these organisms to elevated salt concentrations in the bulk liquid. Even though stable densification was achieved in this case, future research should be conducted focusing on pilot-scale testing. This can lead to insights of system stability, as a higher variation of wastewater composition and salt concentrations will likely occur. Investigation of the microbial community in these saline environments should also be optimized in the future. In conclusion, the implementation of an anaerobic feast/aerobic famine strategy provides a useful and robust solution to overcoming filamentous bulking problems, also in high-salinity petrochemical environments.

FUNDING

This research was funded by the Industrial Research Fund (IOF) of the University of Antwerp through a Proof of Concept (POC) project.

DATA AVAILABILITY STATEMENT

All relevant data are included in the paper or its Supplementary Information.

CONFLICT OF INTEREST

The authors declare there is no conflict.

REFERENCES

APHA 2017 *Standard Methods for the Examination of Water and Wastewater*, 23rd edn. American Public Health Association, Washington, DC.

Caluwé, M., Dobbeleers, T., D'Aes, J., Miele, S., Akkermans, V., Daens, D., Geuens, L., Kiekens, F., Blust, R. & Dries, J. 2017 Formation of aerobic granular sludge during the treatment of petrochemical wastewater. *Bioresource Technology* **238**, 559–567. https://doi.org/10.1016/j.biortech.2017.04.068.

Caluwé, M., Dobbeleers, T., Daens, D., Geuens, L., Blust, R. & Dries, J. 2018 SBR treatment of tank truck cleaning wastewater: sludge characteristics, chemical and ecotoxicological effluent quality. *Environmental Technology* **39** (19), 2524–2533. doi:10.1080/09593330.2017.1359342.

Caluwé, M., Goossens, K., Seguel Suazo, K., Tsertou, E. & Dries, J. 2022 Granulation strategies applied to industrial wastewater treatment: from lab to full-scale. *Water Science and Technology* **85** (9), 2761–2771. doi:10.2166/wst.2022.129.

Carrera, P., Campo, R., Méndez, R., Di Bella, G., Campos, J. L., Mosquera-Corral, A. & Val del Rio, A. 2019 Does the feeding strategy enhance the aerobic granular sludge stability treating saline effluents? *Chemosphere* **226**, 865–873. https://doi.org/10.1016/j.chemosphere.2019.03.127.

Carrera, P., Casero-Díaz, T., Castro-Barros, C. M., Méndez, R., Val del Río, A. & Mosquera-Corral, A. 2021 Features of aerobic granular sludge formation treating fluctuating industrial saline wastewater at pilot scale. *Journal of Environmental Management* **296**, 113135. https://doi.org/10.1016/j.jenvman.2021.113135.

Chiu, Y.-C. & Chung, M.-S. 2003 Determination of optimal COD/nitrate ratio for biological denitrification. *International Biodeterioration & Biodegradation* **51** (1), 43–49. https://doi.org/10.1016/S0964-8305(02)00074-4.

Chung, J. & Bae, W. 2002 Nitrite reduction by a mixed culture under conditions relevant to shortcut biological nitrogen removal. *Biodegradation* **13** (3), 163–170. doi:10.1023/A:1020896412365.

Cornelissen, R., Van Dyck, T., Dries, J., Ockier, P., Smets, I., Van den Broeck, R. & Feyaerts, M. 2018 Application of online instrumentation in industrial wastewater treatment plants – a survey in Flanders, Belgium. *Water Science and Technology* **78** (3–4), 957–967. doi:10.2166/wst.2018.375.

Corsino, S. F., di Biase, A., Devlin, T. R., Munz, G., Torregrossa, M. & Oleszkiewicz, J. A. 2017 Effect of extended famine conditions on aerobic granular sludge stability in the treatment of brewery wastewater. *Bioresource Technology* **226**, 150–157. https://doi.org/10.1016/j.biortech.2016.12.026.

de Graaff, D. R., van Loosdrecht, M. C. M. & Pronk, M. 2020a Biological phosphorus removal in seawater-adapted aerobic granular sludge. *Water Research* **172**, 115531. https://doi.org/10.1016/j.watres.2020.115531.

de Graaff, D. R., van Loosdrecht, M. C. M. & Pronk, M. 2020b Stable granulation of seawater-adapted aerobic granular sludge with filamentous Thiothrix bacteria. *Water Research* **175**, 115683. https://doi.org/10.1016/j.watres.2020.115683.

de Kreuk, M. K. & van Loosdrecht, M. C. M. 2004 Selection of slow growing organisms as a means for improving aerobic granular sludge stability. *Water Science and Technology* **49** (11–12), 9–17. doi:10.2166/wst.2004.0792.

de Kreuk, M. K., Kishida, N., Tsuneda, S. & van Loosdrecht, M. C. M. 2010 Behavior of polymeric substrates in an aerobic granular sludge system. *Water Research* **44** (20), 5929–5938. https://doi.org/10.1016/j.watres.2010.07.033.

Dobbeleers, T., Daens, D., Miele, S., D'aes, J., Caluwé, M., Geuens, L. & Dries, J. 2017 Performance of aerobic nitrite granules treating an anaerobic pre-treated wastewater originating from the potato industry. *Bioresource Technology* **226**, 211–219. https://doi.org/10.1016/j.biortech.2016.11.117.

Dueholm, M. K. D., Nierychlo, M., Andersen, K. S., Rudkjøbing, V., Knutsson, S., Arriaga, S. & Mi, D. A. S. G. C. 2022 MiDAS 4: a global catalogue of full-length 16S rRNA gene sequences and taxonomy for studies of bacterial communities in wastewater treatment plants. *Nature Communications* **13** (1), 1908. doi:10.1038/s41467-022-29438-7.

Edgar, R. C. 2013 UPARSE: highly accurate OTU sequences from microbial amplicon reads. *Nature Methods* **10** (10), 996–998. doi:10.1038/nmeth.2604.

Hamza, R. A., Zaghloul, M. S., Iorhemen, O. T., Sheng, Z. & Tay, J. H. 2019 Optimization of organics to nutrients (COD:N:P) ratio for aerobic granular sludge treating high-strength organic wastewater. *Science of The Total Environment* **650**, 3168–3179. https://doi.org/10.1016/j.scitotenv.2018.10.026.

He, Q., Wang, H., Chen, L., Gao, S., Zhang, W., Song, J. & Yu, J. 2020 Elevated salinity deteriorated enhanced biological phosphorus removal in an aerobic granular sludge sequencing batch reactor performing simultaneous nitrification, denitrification and phosphorus removal. *Journal of Hazardous Materials* **390**, 121782. https://doi.org/10.1016/j.jhazmat.2019.121782.

Jenkins, D., Richard, M. G. & Daigger, G. T. 2003 *Manual on the Causes and Control of Activated Sludge Bulking, Foaming, and Other Solids Separation Problems*, 3rd edn.. CRC Press. https://doi.org/10.1201/9780203503157.

Martins, A. M. P., Pagilla, K., Heijnen, J. J. & van Loosdrecht, M. C. M. 2004 Filamentous bulking sludge – a critical review. *Water Research* **38** (4), 793–817. https://doi.org/10.1016/j.watres.2003.11.005.

Ou, D., Li, W., Li, H., Wu, X., Li, C., Zhuge, Y. & Liu, Y.-d. 2018 Enhancement of the removal and settling performance for aerobic granular sludge under hypersaline stress. *Chemosphere* **212**, 400–407. https://doi.org/10.1016/j.chemosphere.2018.08.096.

Pronk, M., Bassin, J. P., de Kreuk, M. K., Kleerebezem, R. & van Loosdrecht, M. C. M. 2014 Evaluating the main and side effects of high salinity on aerobic granular sludge. *Applied Microbiology and Biotechnology* **98** (3), 1339–1348. doi:10.1007/s00253-013-4912-z.

Ramos, C., Suárez-Ojeda, M. E. & Carrera, J. 2015 Long-term impact of salinity on the performance and microbial population of an aerobic granular reactor treating a high-strength aromatic wastewater. *Bioresource Technology* **198**, 844–851. https://doi.org/10.1016/j.biortech.2015.09.084.

Toja Ortega, S., Pronk, M. & de Kreuk, M. K. 2021 Anaerobic hydrolysis of complex substrates in full-scale aerobic granular sludge: enzymatic activity determined in different sludge fractions. *Applied Microbiology and Biotechnology* **105** (14), 6073–6086. doi:10.1007/s00253-021-11443-3.

van den Akker, B., Reid, K., Middlemiss, K. & Krampe, J. 2015 Evaluation of granular sludge for secondary treatment of saline municipal sewage. *Journal of Environmental Management* **157**, 139–145. https://doi.org/10.1016/j.jenvman.2015.04.027.

van Loosdrecht, M., Nielsen, P., Lopez-Vazquez, C. & Brdjanovic, D. 2016 *Experimental Methods in Wastewater Treatment*. 9781780404752. https://doi.org/10.2166/9781780404752.

Wang, X., Yang, T., Lin, B. & Tang, Y. 2017a Effects of salinity on the performance, microbial community, and functional proteins in an aerobic granular sludge system. *Chemosphere* **184**, 1241–1249. https://doi.org/10.1016/j.chemosphere.2017.06.047.

Wang, Z., van Loosdrecht, M. C. M. & Saikaly, P. E. 2017b Gradual adaptation to salt and dissolved oxygen: strategies to minimize adverse effect of salinity on aerobic granular sludge. *Water Research* **124**, 702–712. https://doi.org/10.1016/j.watres.2017.08.026.

Welles, L., Lopez-Vazquez, C. M., Hooijmans, C. M., van Loosdrecht, M. C. & Brdjanovic, D. 2014 Impact of salinity on the anaerobic metabolism of phosphate-accumulating organisms (PAO) and glycogen-accumulating organisms (GAO). *Applied Microbiology and Biotechnology* **98** (17), 7609–7622. doi:10.1007/s00253-014-5778-4.

First received 10 August 2022; accepted in revised form 25 January 2023. Available online 4 February 2023